Novel Mechanism of Foxo1 Phosphorylation in Glucagon Signaling in Control of Glucose Homeostasis

Yuxin Wu,[1] Quan Pan,[1] Hui Yan,[1] Kebin Zhang,[1] Xiaoqin Guo,[2,3] Zihui Xu,[1] Wanbao Yang,[1] Yajuan Qi,[1] Cathy A. Guo,[1] Caitlyn Hornsby,[1] Lin Zhang,[4] Aimin Zhou,[4] Ling Li,[1] Yunmei Chen,[1] Weiping Zhang,[1] Yuxiang Sun,[1] Hongting Zheng,[2] Fred Wondisford,[3] Ling He,[3] and Shaodong Guo[1]

Diabetes 2018;67:2167–2182 | https://doi.org/10.2337/db18-0674

Dysregulation of hepatic glucose production (HGP) serves as a major underlying mechanism for the pathogenesis of type 2 diabetes. The pancreatic hormone glucagon increases and insulin suppresses HGP, controlling blood glucose homeostasis. The forkhead transcription factor Foxo1 promotes HGP through increasing expression of genes encoding the rate-limiting enzymes responsible for gluconeogenesis. We previously established that insulin suppresses Foxo1 by Akt-mediated phosphorylation of Foxo1 at Ser^{256} in human hepatocytes. In this study, we found a novel Foxo1 regulatory mechanism by glucagon, which promotes Foxo1 nuclear translocation and stability via cAMP- and protein kinase A–dependent phosphorylation of Foxo1 at Ser^{276}. Replacing Foxo1-S276 with alanine (A) or aspartate (D) to block or mimic phosphorylation, respectively, markedly regulates Foxo1 stability and nuclear localization in human hepatocytes. To establish in vivo function of Foxo1-Ser^{276} phosphorylation in glucose metabolism, we generated Foxo1-S273A and Foxo1-S273D knock-in (KI) mice. The KI mice displayed impaired blood glucose homeostasis, as well as the basal and glucagon-mediated HGP in hepatocytes. Thus, Foxo1-Ser^{276} is a new target site identified in the control of Foxo1 bioactivity and associated metabolic diseases.

Glucagon and insulin are the most important pancreatic hormones in target tissues, such as liver, in control of glucose homeostasis in the body in response to food intake (1,2). During the fasting state, glucagon is secreted from the pancreatic α-cells to elevate blood glucose through stimulation of gluconeogenesis and glycogenolysis, protecting the body from hypoglycemia (3). However, an excess of blood glucagon level is present in animals and patients with diabetes, stimulating excessive hepatic gluconeogenesis and contributing to diabetic hyperglycemia (1,4–7).

Glucagon exerts its function through binding to the glucagon receptor (GCGR), a G-protein–coupled receptor. Upon binding to glucagon, GCGR in the cell membrane activates adenylate cyclase to elevate intracellular cAMP and subsequently activates protein kinase A (PKA) signaling (1,2). PKA regulates the metabolic enzymes or gene expression for glycogenolysis and gluconeogenesis, including glycogen phosphorylase, glucose-6-phosphatase catalytic subunit (G6pc), and phosphoenolpyruvate carboxykinase-1 (Pck1) (8), increasing blood glucose. Importantly, recent studies demonstrated that inhibition of GCGR by a genetic approach or chemical administration in mice significantly decreases the blood glucose and completely prevents streptozotocin-induced hyperglycemia in type 1 diabetes (1), suggesting that glucagon-mediated hepatic glucose production (HGP) or gluconeogenesis is a potential target for therapeutic intervention of diabetes (9,10).

Gluconeogenesis is suppressed by insulin involved in the gene transcriptional regulation in the nucleus. Foxo1, a member of the Foxo family, is an important component of insulin-signaling cascades in regulating cellular growth, differentiation, and metabolism (11). Our and other studies demonstrated that Foxo1 enhances gene transcription

[1]Department of Nutrition and Food Science, College of Agriculture and Life Sciences, Texas A&M University, College Station, TX
[2]Department of Endocrinology, Third Military Medical University, Chongqing, China
[3]Division of Endocrinology, Department of Medicine, Johns Hopkins University, Baltimore, MD
[4]Department of Chemistry, Cleveland State University, Cleveland, OH
Corresponding author: Shaodong Guo, shaodong.guo@tamu.edu.

Received 18 June 2018 and accepted 21 August 2018.
This article contains Supplementary Data online at http://diabetes.diabetesjournals.org/lookup/suppl/doi:10.2337/db18-0674/-/DC1.
Y.W., Q.P., H.Y., and K.Z. contributed equally to this work.

of the rate-limiting enzymes responsible for gluconeogenesis, including G6pc and Pck1, through interaction with a conserved insulin-responsive element on the promoter region of the target genes (12–14), and increases HGP (11,15–17). However, insulin suppresses Foxo1 by the insulin receptor substrate 1 and 2 (IRS1 and 2)–dependent activation of Akt that phosphorylates Foxo1 at Ser^{256} in human hepatocytes, which is equivalent to mouse Foxo-S253, promoting Foxo1 nuclear export and/or degradation and then decreasing HGP and blood glucose (18–21).

Foxo1 protein is stabilized in the liver of fasting mice when insulin decreases and glucagon increases in the blood circulation. Our early studies indicate that Foxo1 may partially mediate the effect of cAMP, a second messenger of glucagon, or glucocorticoid-induced expression of genes encoding gluconeogenic enzymes, such as G6pc and Pck1 (22,23). Recently, a calcium-sensing enzyme, Ca^{2+}/calmodulin-dependent protein kinase II (CaMKII), is shown to increase seven non-Akt phosphorylation sites of Foxo1, mediating the action of glucagon and cAMP signaling and enhancing Foxo1 nuclear localization and HGP, but detailed phosphorylation sites involved in glucagon or cAMP signaling remain elusive in vivo (24). In this study, we hypothesize that Foxo1 may play a role in the action of glucagon in control of HGP or gluconeogenesis and investigated the molecular and physiological mechanism of Foxo1 regulation by glucagon via PKA with the aim of better understanding the fundamentals of blood glucose homeostasis and pathogenesis of diabetes.

RESEARCH DESIGN AND METHODS

In Vitro Kinase Assay and Liquid Chromatography–Mass Spectrometry

To determine whether Foxo1 is directly phosphorylated by PKA, we performed in vitro kinase assay, in which 20 μg of recombinant Foxo1–glutathione-*S*-transferase (GST) fusion protein was purchased from Millipore Inc. as previously described (18). The purified Foxo1-GST recombinant protein was incubated with 5 units of recombinant catalytic subunit of PKA (PKAc; Upstate Biotechnology) for 1 h, at 30°C, in 50 μL reaction buffer (25 mmol/L Tris-HCl, pH 7, 1 mmol/L EGTA, 0.5 mmol/L EDTA, 0.5 mmol/L β-mercaptoethanol, and 3 mmol/L magnesium acetate) with or without 0.1 mmol/L ATP. The protein bands of interest in the SDS-PAGE gel were incised and prepared for liquid chromatography–mass spectrometry (LC-MS) analysis, as described in the Supplementary Data.

DNA Mutagenesis

Plasmid DNA expressing human Foxo1-WT (wild-type) was previously described (12). Oligos specific for human Foxo1-S153A, Foxo1-S153D, Foxo1-S276A, or Foxo1-S276D were designed, the QuickChange Site-Directed Mutagenesis kit was purchased (Stratagene, La Jolla, CA), and mutant sites were confirmed by DNA sequencing.

Mice

All animal experiments were performed according to procedures approved by the Texas A&M University Institutional Animal Care and Use Committee. The floxed Foxo1 mice ($Foxo1^{L/L}$) (25) and albumin-Cre mice were previously described (26). All of the mice on a C57BL/6 and 129 Sv mixed background were maintained on regular chow (Isopro 5P76; Prolab). Foxo1-S273A and Foxo1-S273D knock-in (KI) mice were generated using the CRISPR/Cas9 approaches (27) and the microinjection and mouse colonies production performed by Cyagen Biosciences Inc. (Santa Clara, CA; contract number: NTMCN-150310-AML-01). The founder mice were backcrossed to C57/BL6 mice, and F3 offspring male mice were used for analysis. The tail DNA of pups was genotyped by PCR and then confirmed by DNA sequencing analysis. The *db/db* mice were purchased from The Jackson Laboratory (Bar Harbor, ME). If not specified elsewhere, all of the mice were male at the ages of 8–12 weeks. For the high-fat diet (HFD)–induced insulin-resistant mouse model, 8–10-week-old male mice were fed with HFD (42% kcal from fat, TD.88137; Envigo) or control low-fat diet (LFD; 13% kcal from fat, TD08485; Envigo) for 6 months. For glucagon-tolerant tests, mice after an 18-h fast were i.p. injected with glucagon of 16 μg/kg body weight, and blood glucose was measured with a glucometer (Elite XL; Bayer). The dose of glucagon used was based on a recent report (28).

Generation of Phosphospecific Antibodies for Foxo1

We synthesized two peptides of human Foxo1 corresponding to residues 143–162 (GPLAGQPRKSpSSSRRNAWGN) and 265–285 (KSRSRAAKKKApSLQSGQEGAG), where "p" indicates the site of phosphorylation (S153 and S276). The peptides were conjugated to both keyhole limpet hemocyanin and BSA and used to immunize rabbits at Covance (Denver, PA; Custom Immunology Service, CRPQ20383-01P), as previously described (18).

Blood Chemistry and Metabolic Analysis

Serum was analyzed for insulin (Crystal Chem) and glucagon (Alpco) using commercial protocol and reagents. Blood glucose was measured using a glucometer (Bayer). For glucagon stimulation experiments, 8–12-week-old mice were subjected to an 18-h fasting, injected i.p. by glucagon (pharmaceutical grade, 0.25 mg/kg body weight), and blood glucose monitored. For GCGR antagonist injection, 6-h fasted control mice were i.v. injected with GCGR antagonist ([des-His^1, Glu^9]-glucagon amide; 1 mg/kg body weight).

Protein Analysis and Western Blotting

Proteins were prepared from cells or livers, resolved by SDS-PAGE, and transferred to nitrocellulose membrane for immunoblotting analysis using specific antibodies, as previously described (29). The signal intensity was measured and analyzed by ImageJ software (National Institutes of Health).

Nuclear and Cytoplasmic Protein Extraction

Nuclear and cytoplasmic proteins from HepG2 or liver tissue were extracted with NE-PER nuclear (NER) and cytoplasmic (CER-I and CER-II) extraction reagent (Pierce), as previously described (29).

Gluconeogenesis, Glycogenolysis, and HGP Assay

The primary mouse hepatocytes were isolated from 8–12-week-old mice via 0.05% collagenase (type 1; Worthington Biochemical) and cultured as previously described (16). For HGP assays, freshly isolated hepatocytes were resuspended in DMEM with 2% FBS for 4 h, then rinsed with PBS, and cultured in HGP buffer (118 mmol/L NaCl, 2.5 mmol/L $CaCl_2$, 4.8 mmol/L KCl, 25 mmol/L $NaHCO_3$, 1.1 mmol/L KH_2PO_4, 1.2 mmol/L $MgSO_4$, 10 μmol/L $ZnSO_4$, 0.6% BSA, 10 mmol/L HEPES, 10 mmol/L sodium DL-lactate, and 5 mmol/L pyruvate, pH 7.4) in the presence or absence of 100 nmol/L glucagon or 8-Br–cAMP. Cell culture medium was collected at 3 and 6 h and glucose in the medium measured according to the manufacturer's protocol using Amplex Red Glucose Assay (Invitrogen) (30,31). For glycogenolysis assay, lactate and pyruvate in the HGP buffer were removed and glucose release into the medium measured after treatments.

Quantitative Real-time PCR

RNA was extracted with TRIzol reagent (Invitrogen), cDNA synthesis used the Super-Script first-strand synthesis system (Bio-Rad), and gene expression was measured with the SYBR Green Supermix system (Bio-Rad), as previously described (29).

Gene Transfection and Luciferase Reporter Gene Assay and Confocal Fluorescent Microscope

HepG2 cells were cultured with DMEM with 10% FBS for 6 h. Cell cultures were then subjected to Lipofectamine 3000 (Life Technologies) with plasmids according to the manufacturer's instruction. The dual-luciferase reporter assay system from Promega was purchased, luciferase activity measured with an Optocomp-I luminometer (MGM Instruments), and cells expressing eGFP and eGFP-Foxo1 visualized with the confocal microscope (Leica Biosystems) and calculated as previously described (32).

Statistical Analysis

The comparison of differences between two groups was performed using a Student two-tailed *t* test to determine the significance (26). ANOVA tests were used when comparing two groups among multiple groups. All data are presented as mean ± SEM. A *P* value <0.05 was considered statistically significant.

RESULTS

Hepatic Foxo1 Is Involved in Glucagon-Induced Glucose Production in Mice

Previous studies from our group and others have shown that liver-specific Foxo1 knockout mice (L-F1KO) or hepatic Foxo1 suppression exhibited a 15–20% reduction in blood glucose as compared with control mice (16,17,33). To determine whether Foxo1 is involved in the action of glucagon-mediated blood glucose homeostasis, we administered glucagon i.p. in L-F1KO and control-fed mice. Glucagon significantly increased blood glucose by 32% in control mice 60 min after glucagon injection, but the increased potential in L-F1KO mice was 21%, with a significant reduction compared with control mice (Fig. 1*A*). We next performed the glucagon tolerance test in the mice in the fasting state. Both control and L-F1KO mice exhibited an ~1.7-fold elevation in blood glucose 15 min after glucagon injection. Importantly, the ability of blood glucose increase was maintained in 60 min after glucagon injection in control mice; however, L-F1KO mice exhibited a 50% reduction in blood glucose after glucagon stimulation compared with control mice ($P < 0.05$) (Fig. 1*B*). Gene expression analysis indicated that glucagon stimulated hepatic gene transcriptional levels of Igfbp-1, G6pc, and Pck1 in control mice by 4.4-, 2.6-, and 2.0-fold, respectively. However, glucagon stimulation on Igfbp-1, G6pc, and Pck1 was 3.2-, 2.0-, and 1.8-fold, respectively, in L-F1KO liver, exhibiting significant reductions compared with control (Fig. 1*C–E*).

To determine whether Foxo1 deficiency impairs glucagon-mediated glucose production via glycogenolysis and gluconeogenesis in an autonomous manner in hepatocytes, we measured HGP with glucagon treatment in primary hepatocytes isolated from L-F1KO and control mice. Glucagon significantly increased HGP by 42% in control hepatocytes and by 35% in L-F1KO hepatocytes, exhibiting a 28% reduction in L-F1KO cells (Fig. 1*F*). Both glycogenolysis and gluconeogenesis contribute to HGP; L-F1KO cells exhibited a 50% reduction in glucagon-stimulated gluconeogenesis compared with control (46% stimulation in control vs. 23% in L-F1KO; $P < 0.01$). Glucagon significantly increased glycogenolysis by 21% in control cells; L-F1KO hepatocytes had no blockage for glucagon, even though the basal level of glycogenolysis was 29% lower in L-F1KO than control cells (71 ± 4.2 μmol/h/g protein vs. 50 ± 4.9 μmol/h/g protein; $P < 0.01$) (Fig. 1*F*). Taken together, these data indicate that Foxo1 deficiency impaired glucagon-induced liver gene expression, gluconeogenesis, and blood glucose.

Insulin and Glucagon Exhibit an Opposite Effect on Foxo1 Stability in Hepatocytes

We next examined the effect of insulin versus glucagon on Foxo1 regulation in hepatocytes. HepG2 cells were cultured and treated the hormones over a 6-h time course. Insulin treatment for 3 h significantly reduced total Foxo1 protein by 20%. However, glucagon treatment for 3 h significantly increased total Foxo1 protein by 1.7-fold (Fig. 2*A* and *B*). The phosphorylation level of Foxo1 at S256 was increased 2.5-fold by insulin for 3-h treatment and persisted up to 6 h, whereas glucagon barely stimulated Foxo1-S256 phosphorylation even that the

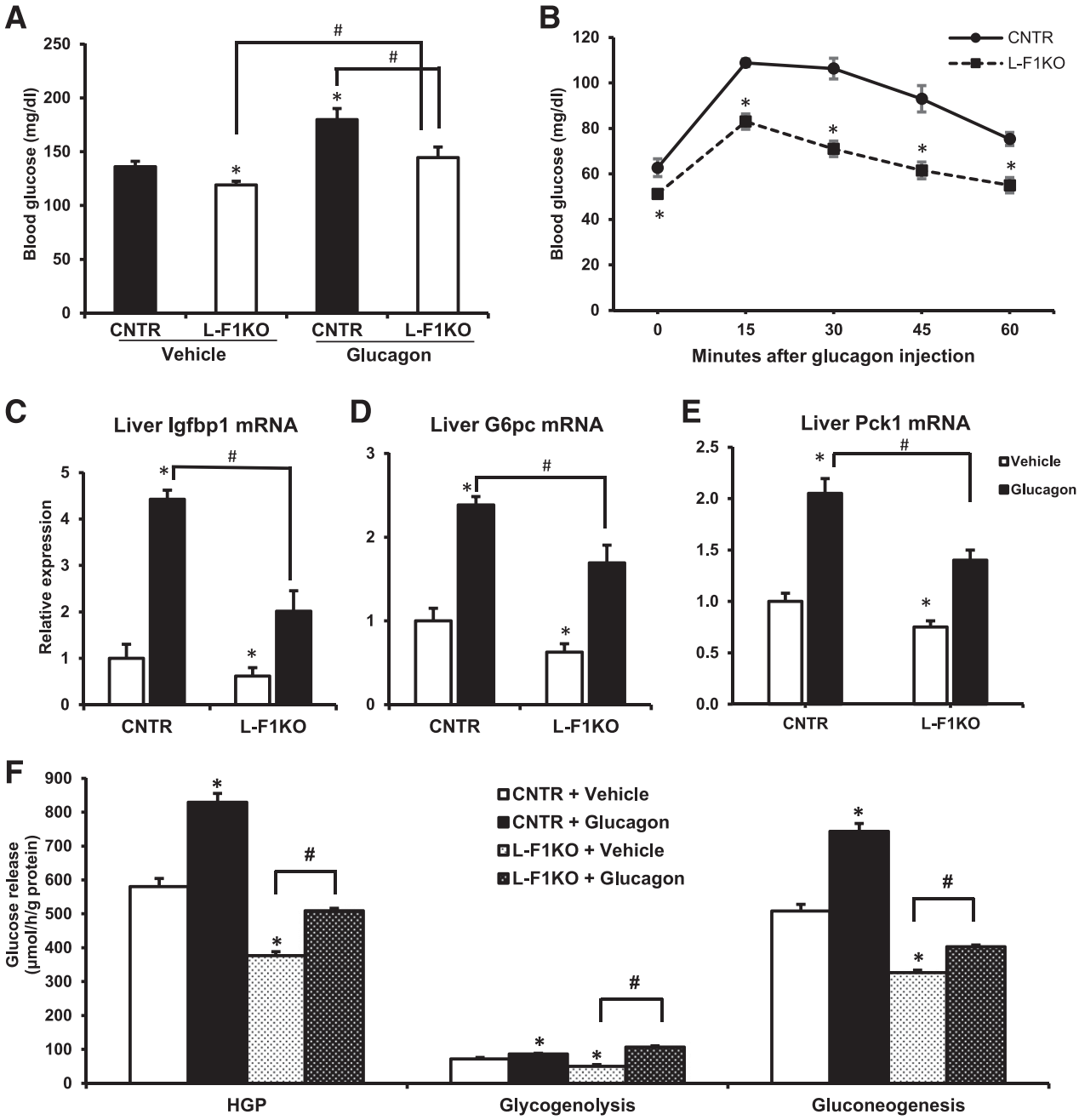

Figure 1—The effect of hepatic Foxo1 deletion on glucagon-induced glucose production and gluconeogenesis. *A*: Blood glucose level in random-fed mice in 1 h after i.p. injection of 0.25 mg/kg body weight glucagon. Ten-week-old mice per treatment. $n = 6$ mice/group. *$P < 0.05$ vs. control mice (CNTR); #$P < 0.05$ for the comparison of designated groups. *B*: Glucagon tolerance tests for mice after an 18-h overnight fast. Blood glucose levels (mean ± SEM) were determined at the indicated time points after i.p. injection of 16 μg/kg body weight glucagon. $n = 6$ mice/group. *$P < 0.05$ vs. CNTR. *C–E*: Quantitative RT-PCR analyses of the livers of mice with i.p. injection of 0.25 mg/kg body glucagon for 1 h. $n = 3$ mice/treatment. *$P < 0.05$ vs. CNTR; #$P < 0.05$ for the comparison of designated groups. *F*: HGP, glycogenolysis, and gluconeogenesis in primary hepatocytes. Cells were isolated from WT or L-F1KO mice, cultured in DMEM with 2% FBS medium for attachment for 4 h, and then switched to HGP buffer with or without pyruvate substrate. HGP was measured 3 h after 100 nmol/L glucagon stimulation and normalized to total protein levels. $n = 3$/group. *$P < 0.05$ vs. CNTR; #$P < 0.05$ vs. L-F1KO.

phosphorylation was slightly reduced at 3 h of treatment (Fig. 2*A* and *C*). Insulin treatment for 15 min increased by 23-fold on Akt phosphorylation at T308, which was increased 5-fold by glucagon when compared with the basal level of Akt phosphorylation in cells (Fig. 2*A* and *D*). By contrast, insulin barely increased phosphorylation of CREB at S133, a target of PKA, but glucagon treatment for 15 min significantly increased CREB-S133 phosphorylation by 1.5-fold without changing the total CREB protein level (Fig. 2*A*, *B*, and *E*). Moreover, Foxo1 mRNA levels

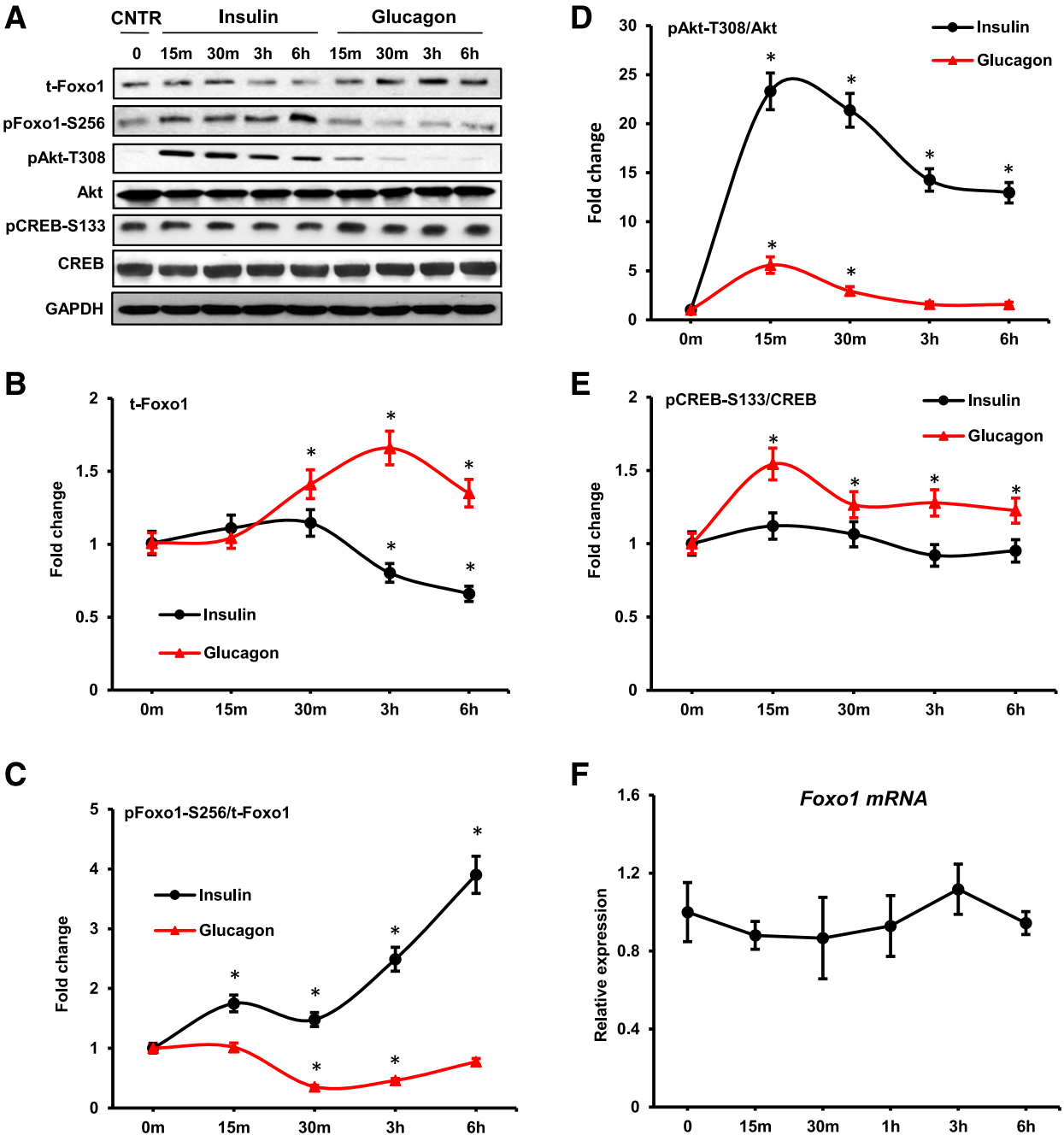

Figure 2—Regulation of Foxo1 stability and activity by insulin and glucagon in hepatocytes. *A*: Insulin and glucagon signaling in HepG2 cells. Cells were cultured in DMEM with 10% FBS and then starved in DMEM with 1% BSA medium overnight prior to the treatment of 100 nmol/L insulin or 100 nmol/L glucagon over a 6-h time course. Western blotting was performed with 150 μg protein of cell lysates to detect total Foxo1 (t-Foxo1), Akt, CREB, phosphorylated (p)Foxo1-S256, pAkt-T308, and pCREB-S133. Quantification of t-Foxo1/GAPDH (*B*), pFoxo1-S256/t-Foxo1 (*C*), pAKT-T308/Akt (*D*), and pCREB-S133/CREB (*E*) from *A* was performed using ImageJ. Results are presented as mean ± SEM. *$P < 0.05$ vs. 0-min treatment. $n = 3$ experiments. *F*: The mRNA expression of *Foxo1* in HepG2 cells. HepG2 cells were cultured in DMEM with 10% FBS and then starved in DMEM with 1% BSA medium overnight prior to the treatment of 100 nmol/L glucagon over a 6-h time course. The Foxo1 mRNA level was detected by quantitative PCR. $n = 3$ experiments. CNTR, control.

were unaffected by glucagon in HepG2 cells (Fig. 2*F*). These results prompted us to hypothesize that glucagon may promote Foxo1 stability through activation of PKA and control Foxo1 target gene expression, impelling us to assess the impact of Foxo1 in glucagon-regulated HGP in vivo.

PKA Stimulates and Akt Inhibits the Foxo1-Regulated Reporter Gene Activity

PKA and Akt serve as important downstream effectors in glucagon and insulin signaling, respectively, in control of glucose homeostasis (15,34). In order to determine whether PKA affects Foxo1-mediated gene

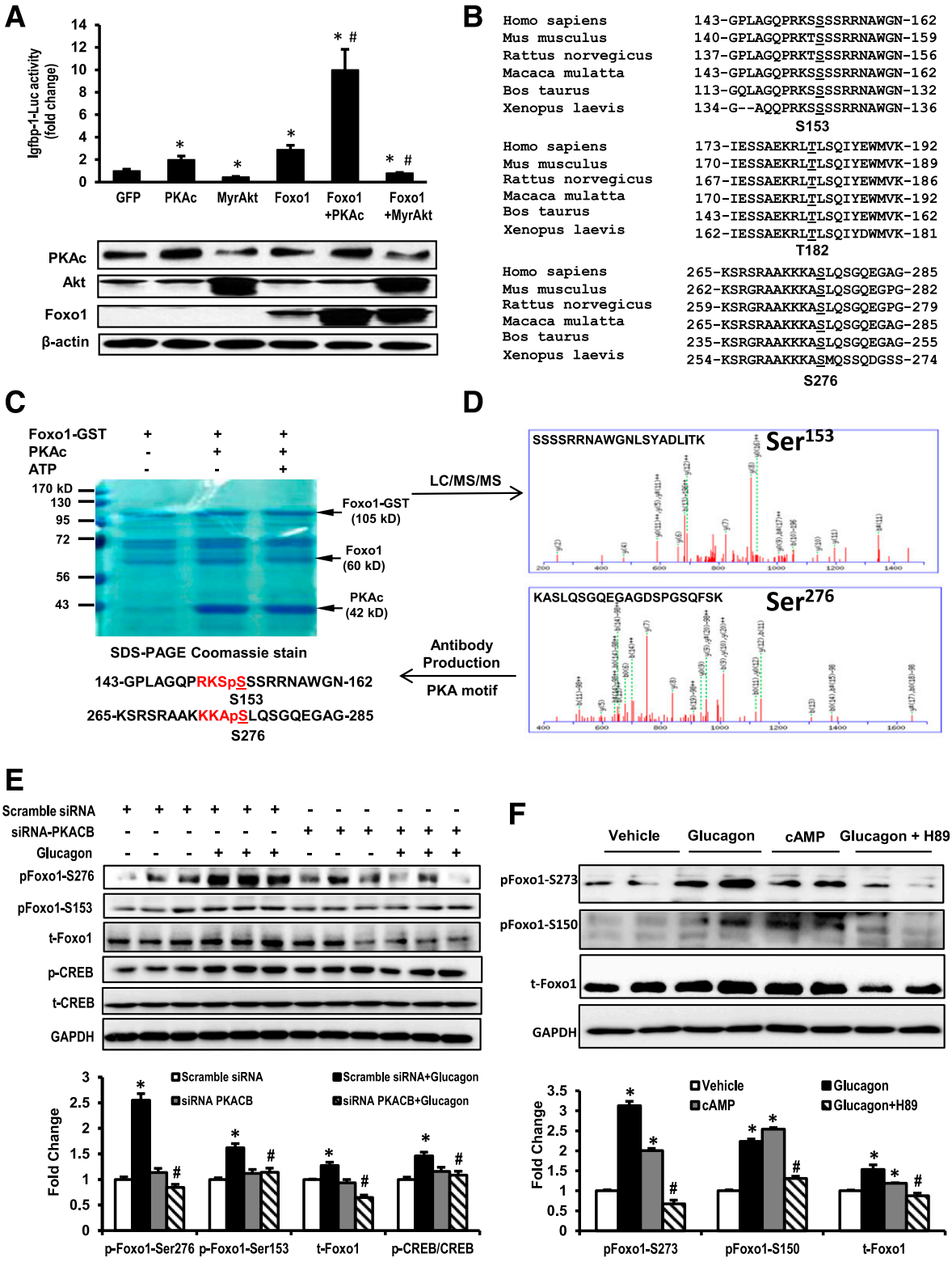

Figure 3— Identification of novel phosphorylation sites of Foxo1 by PKA. *A*: PKA activates and Akt inhibits Igfbp-1 promoter activity in cells. HepG2 cells were cultured in a six-well plate with DMEM with 10% FBS and then transfected with 0.5 μg Igfbp-1–Luc reporter gene and 0.1 μg RL-luc internal control together with 0.5 μg expression vector for GFP, PKAc, Myr-Akt, hemagglutinin (HA)-Foxo1, or a combination of the two as designated. Cell lysates were prepared for luciferase assays and protein levels of PKA, Akt, Foxo1, or β-actin determined by Western blotting from 20 μg of total protein. $n = 3$ experiments. Values are fold changes of luciferase activity relative to GFP group and presented as mean ± SEM. *$P < 0.05$ vs. GFP; #$P < 0.05$ vs. Foxo1. *B*: Putative phosphorylation sites of Foxo1 by PKA among different species. *C*: PKA phosphorylates Foxo1 in vitro. A total of 20 μg of recombinant Foxo1-GST was mixed with 5 units (0.5 μg) recombinant active PKAc with or without 0.1 mmol/L ATP for 30 min at 30°C and then the Foxo1-GST and PKAc were resolved in SDS-PAGE after the Coomassie Brilliant Blue staining. The intact Foxo1-GST (105 kDa) or cleaved Foxo1 (60 kDa) was incised from the gel and subjected to

transcriptional activity in hepatocytes, we transfected HepG2 cells with the Igfbp-1–luciferase reporter gene construct with plasmid DNA expressing control GFP, PKAc, or constitutively active Akt (Myr-Akt), and then luciferase activities were measured. Overexpression of PKAc alone increased the basal promoter activity by at least twofold, whereas overexpression of the active form of Akt (MyrAkt) inhibited the promoter activity by 55% (Fig. 3*A*). Moreover, expression of Foxo1 alone increased Igfbp-1 promoter activity by 2.9-fold, and coexpressing PKAc and Foxo1 resulted in a robust increase of Igfbp-1 promoter activity, at least by >10-fold. By contrast, co-overexpression of Myr-Akt and Foxo1 almost completely diminished the Foxo1-stimulated Igfbp-1 promoter activity (Fig. 3*A*). Together, these data suggest that PKA had an additive effect on promoting Foxo1-stimulated Igfbp-1 promoter activity.

Identification of Novel Serine/Threonine Phosphorylation Sites of Foxo1 by PKA

Analysis of Foxo1 phosphorylation sites (https://scansite4.mit.edu/4.0/#home) revealed that human Foxo1 contains three PKA consensus sequences (R/KXR*T/S*, R is arginine, K is lysine, and X is any amino acid), located at Ser^{153}, Thr^{182}, and Ser^{276}, which are evolutionarily conserved across species (Fig. 3*B*). We hypothesize that glucagon-activated PKA phosphorylates Foxo1 via these putative PKA phosphorylation sites and enhances Foxo1 stability and transcriptional activity.

Next, we performed an in vitro kinase assay to determine whether PKA can directly phosphorylate Foxo1. GST–fused Foxo1 (Foxo1-GST) and active PKAc were incubated in a protein kinase assay buffer system and then resolved by SDS-PAGE followed by the Coomassie Brilliant Blue staining. Phosphorylated Foxo1 fragment (60 kDa) by PKAc slightly upshifted in mobility (Fig. 3*C*). The Foxo1-GST protein (105 kDa) and Foxo1 fragment (60 kDa) were incised from the gel and subjected to LC–tandem MS (MS/MS) analyses. The results from Mascot analysis of MS of PKAc with or without ATP-treated samples indicated a presence and high score for Foxo1-S276 phosphorylation, a low score for Foxo1-S153 phosphorylation, and no presence and score for T182 phosphorylation (Fig. 3*D*). Based on these results, we generated the phosphospecific antibody against human Foxo1-S276 or Foxo1-S153, which is equivalent to mouse Foxo1-S273 or S150, respectively. In HepG2 cells, glucagon significantly stimulated the phosphorylation of Foxo1-S273 and S153 by 2.5- and 1.5-fold, respectively (Fig. 3*E*). The phosphorylation of S276 and S153 by glucagon was blocked when PKA catalytic subunit C was knocked down by small interfering RNA (siRNA) (Fig. 3*E*). The knockdown of PKA markedly decreased glucagon-stimulated CREB phosphorylation and Foxo1 protein level, suggesting that PKA is essential for maintaining Foxo1 protein stability (Fig. 3*E*). We further confirmed these findings in mouse primary hepatocytes; glucagon treatment enhanced the phosphorylation of Foxo1 at S273 and S150, as well as total Foxo1 protein levels, whereas these effects of glucagon were abolished in the cells when treated with H89, a PKA chemical inhibitor (Fig. 3*F*). In mouse liver, glucagon injection resulted in a 3.8-fold increase in Foxo1-S273 phosphorylation and a 1.6-fold increase in Foxo1-S150 phosphorylation (Fig. 4*A*). Moreover, we administered GCGR antagonist into WT mice and examined whether endogenous Foxo1 protein level is regulated by the glucagon receptor in the liver. Intravenous injection of GCGR antagonist ([des-His^1, Glu^9]-Glucagon amide) resulted in a 20% decrease in blood glucose (Fig. 4*B* and *C*), as well as a 60% decrease of CREB phosphorylation, 55% decrease in Foxo1-S273 phosphorylation, and 35% decrease in total Foxo1 protein level, whereas Foxo1-S150 phosphorylation was barely affected compared with vehicle treatment (Fig. 4*D*). These results suggest that glucagon signaling via its receptor and PKA stimulates hepatic Foxo1 phosphorylation at S273, enhancing Foxo1 stability.

Human Foxo1-S276 Phosphorylation Promotes Foxo1 Nuclear Localization

We next examined whether the newly identified Foxo1 phosphorylation sites play a role in Foxo1 nuclear/cytoplasmic trafficking and stability in cells. We generated plasmid DNA expressing GFP-Foxo1-WT, GFP-Foxo1-S153A, or GFP-Foxo1-S276A, in which serine residue was substituted with an alanine (A) at S153 or S276 to block phosphorylation, whereas GFP-Foxo1-S153D or GFP-Foxo1-S276D containing an aspartate (D) substitution to mimic phosphorylation by introduction of a negative charge. HepG2 cells were transfected with one of these plasmids and then stimulated with 8-Br–cAMP for 15 min prior to confocal imaging. In cells that overexpressed Foxo1-WT, Foxo1 localized in both cytoplasm and nucleus at the basal level, but cAMP stimulation promoted Foxo1 nuclear localization. However, cAMP-induced Foxo1

LC-MS/MS. *D*: MS/MS spectra of peptide containing S153 and S276 of Foxo1. Antibodies against phosphorylated Foxo1 at S153 and S276 were generated. *E* and *F*: Phosphorylation of Foxo1-S276 and S153 by glucagon in cells. *E*: HepG2 cells were transfected with either scramble siRNA or siRNA–PKA catalytic subunit C (PKACB) for 24 h and then treated with or without 100 nmol/L glucagon for 60 min. Quantification of total Foxo1 (t-Foxo1), phosphorylated (p)Foxo1-S276, pFoxo1-S153, pCREB, and CREB was performed using ImageJ and normalized by GAPDH. *$P < 0.05$ vs. scramble siRNA; #$P < 0.05$ vs. scramble siRNA + glucagon. $n = 3$ experiments. *F*: Primary hepatocytes were cultured and treated with either 100 nmol/L glucagon or 10 μmol/L 8-Br–cAMP for 30 min or 10 μmol/L PKA inhibitor H89 for 30 min prior to 60 min of 100 nmol/L glucagon treatment. Phosphorylation of Foxo1-S150 and S273 were analyzed by Western blotting using antibodies at 1:500 dilution. Quantification of pFoxo1-S273, pFoxo1-S150, and t-Foxo1 was performed using ImageJ and normalized by β-actin. n = 3 experiments. *$P < 0.05$ vs. vehicle; #$P < 0.05$ vs. glucagon.

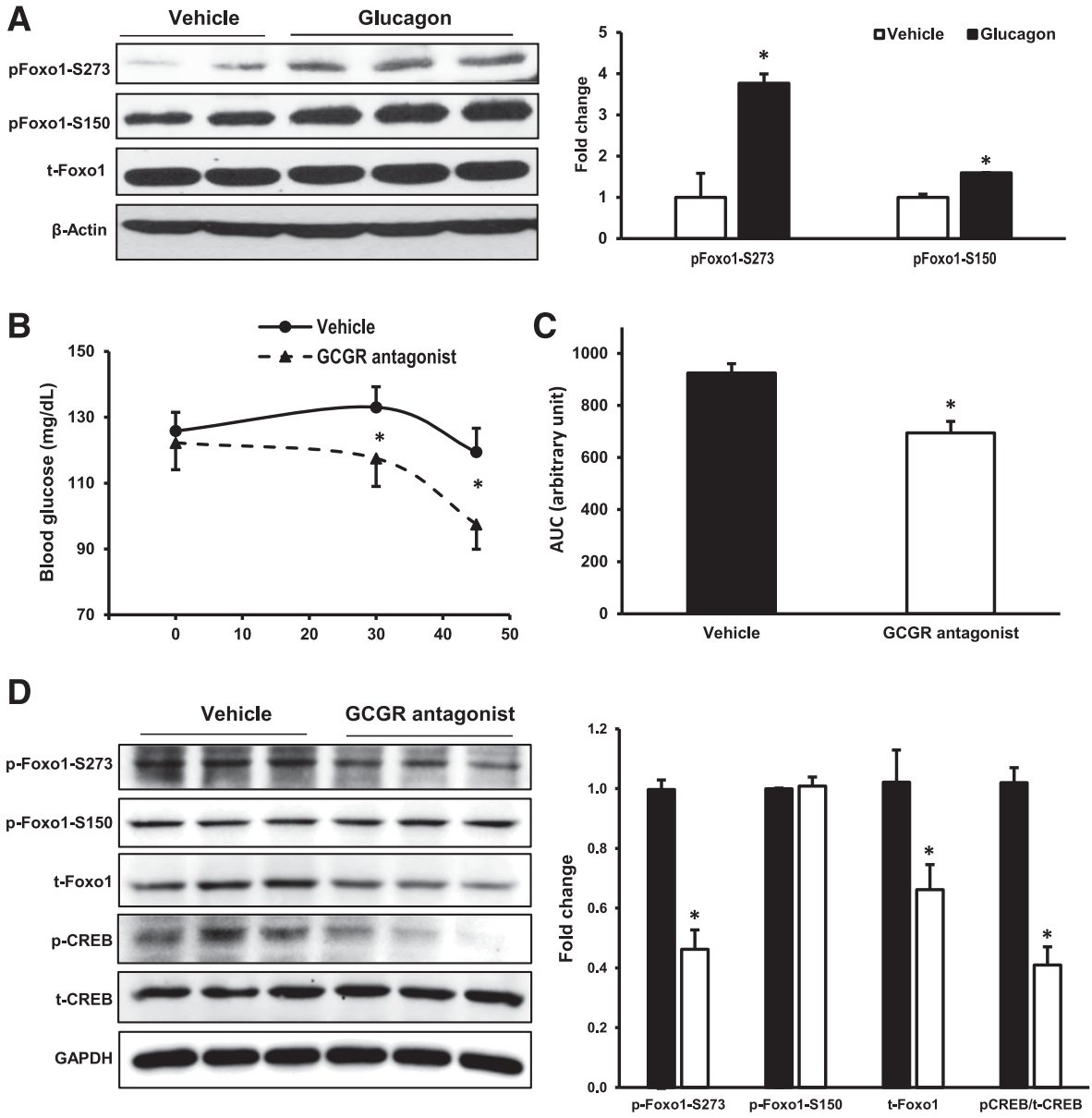

Figure 4—Glucagon promotes phosphorylation of Foxo1-S153 and S276 in vivo. *A*: Random-fed mice were i.p. injected with glucagon at 0.25 mg/kg body weight, and the liver was collected 15 min after injection to determine hepatic Foxo1 phosphorylation at S150 and S273 by using Western blotting. Quantification of phosphorylated (p)Foxo1-S273 and pFoxo1-S150 was performed using ImageJ and normalized by β-actin. $^*P < 0.05$ vs. vehicle. n = 4–6 mice/group. *B–D*: Eight-week-old WT mice were i.v. injected with GCGR antagonist ([des-His^1, Glu^9]-Glucagon amide; 1 mg/kg body weight) after 6 h fasting. *B*: Blood glucose level was measured at the indicated time points. $^*P < 0.05$ vs. vehicle. n = 4–6 mice/group. *C*: Area under the curve (AUC) from *B* was calculated. $^*P < 0.05$ vs. vehicle. n = 4–6 mice/group. *D*: Liver was collected 45 min after [des-His^1, Glu^9]-Glucagon amide injection to determine hepatic total Foxo1 (t-Foxo1) and Foxo1 phosphorylation at S150 and S273 by using Western blotting. Quantification of t-Foxo1, pFoxo1-S273, pFoxo1-S150, pCREB, and CREB was performed using ImageJ and normalized by GAPDH. $^*P < 0.05$ vs. vehicle. n = 4–6 mice/group.

nuclear localization was blocked by S276A mutation, in which overexpressed Foxo1-S276A dispersed primarily within the cytoplasm. Conversely, Foxo1-S276D primarily localized in the nucleus (Fig. 5). Compared with Foxo1-WT, Foxo1-S153A or S153D did not exhibit distinct differences in Foxo1 subcellular localization in cells, and overexpressed Foxo1-S153A and 153D were primarily located to the nucleus in responses to cAMP, similar to Foxo1-WT (Fig. 5). Thus, these results suggest that Foxo1-S276 phosphorylation is crucial for mediating cAMP-stimulated Foxo1 nuclear localization.

To confirm the Foxo1 subcellular localization upon glucagon or cAMP stimulation, we extracted nuclear and cytoplasmic protein from cells for Foxo1 analysis. Glucagon or cAMP stimulated endogenous Foxo1 nuclear localization by nearly threefold compared with vehicle control group (Fig. 6*A*) ($P < 0.05$). By contrast, insulin reduced nuclear total Foxo1 by 25% (Fig. 6*A*). These data indicate

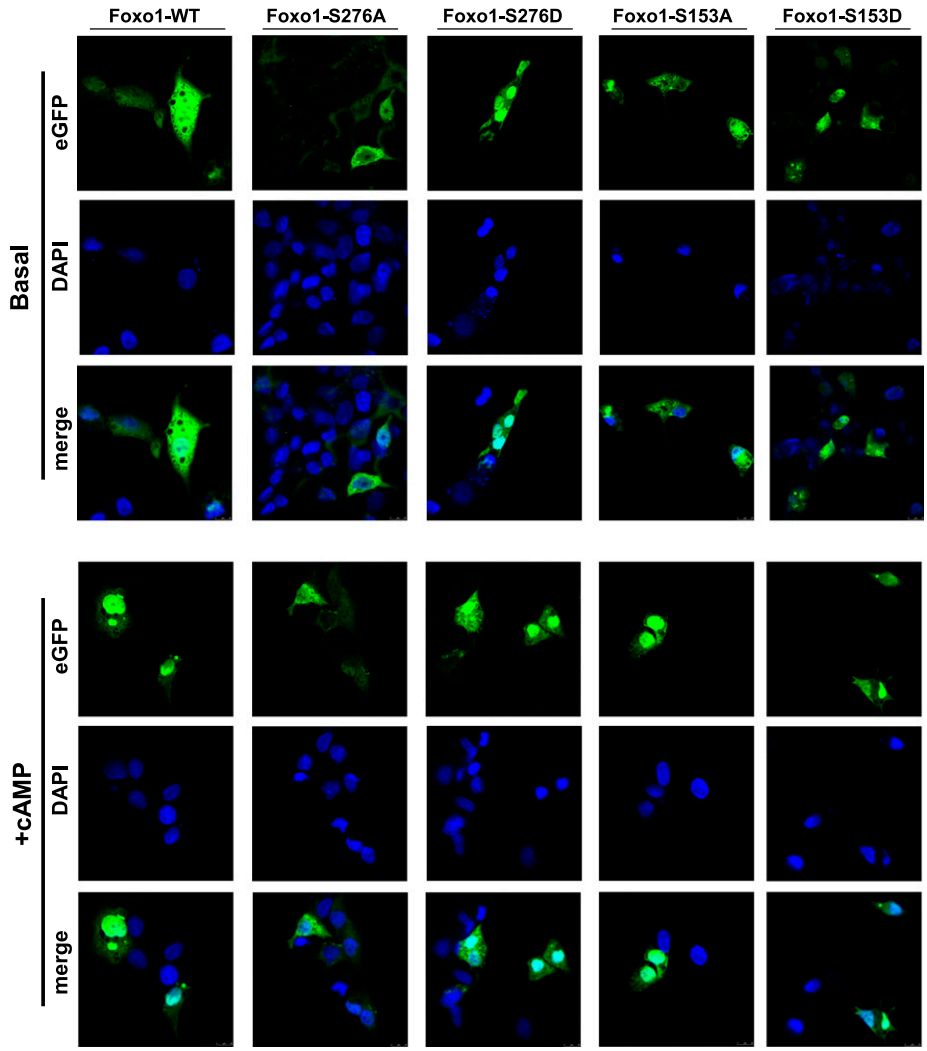

Figure 5—Foxo1-S276 phosphorylation controls cAMP-induced Foxo1 nuclear localization in hepatocytes. HepG2 cells were transfected with 5 μg plasmid DNA expressing GFP-Foxo1-WT, S276A, S276D, S153A, or S153D for 18 h and then treated with or without 10 μmol/L cAMP for 30 min. GFP-positive cells were displayed, stained with DAPI for nucleus, and analyzed under confocal microscope. Representative images are shown.

that either glucagon or cAMP induced Foxo1 nuclear localization, which is distinct from insulin.

Foxo1-S276 Phosphorylation Enhances Foxo1 Stability in Cells

We next further focused on Foxo1-S276 phosphorylation in control of Foxo1 stability in cells. HepG2 cells were transfected with plasmid DNA that expresses Foxo1-WT, Foxo1-S276A, or Foxo1-S276D and then stimulated with glucagon for 30 min followed by nuclear and cytoplasmic protein extraction. In Foxo1-WT–transfected cells, glucagon increased total Foxo1 protein in the nucleus by 1.5-fold (Fig. 6*B* and *C*). Importantly, Foxo1-S276D protein, which mimics S276 phosphorylation with introduction of a negative charge, increased total Foxo1 protein abundance in both nucleus and cytoplasm, mimicking the effect of glucagon on Foxo1 nuclear localization (Fig. 6*B*). By contrast, Foxo1-S276A, which contains a substitution of alanine, largely prevented glucagon-stimulated Foxo1 nuclear localization (Fig. 6*C*).

To further examine the mechanism of Foxo1-S276 phosphorylation in control of Foxo1 stability, we transfected with an equal amount of Foxo1 gene construct with HepG2 cells and then treated cells for 8 h with MG132, a 26*S* proteasome complex inhibitor, preventing Foxo1 protein ubiquitination or cycloheximide (CHX), a protein synthesis inhibitor, inhibiting Foxo1 protein synthesis. When Foxo1-WT, Foxo1-S276A, or Foxo1-S276D plasmid DNA was transfected, the total Foxo1 protein in Foxo1-S276A group was reduced by 50% compared with overexpressed Foxo1-WT ($P < 0.05$) (Fig. 6*D*). However, in the MG132-treated group, the reduction of Foxo1-S276A protein was totally prevented, Foxo1-S276A protein was restored and stabilized to a normal level when compared with Foxo1-WT, and there was no significant difference in total Foxo1 protein levels observed in all of the cells

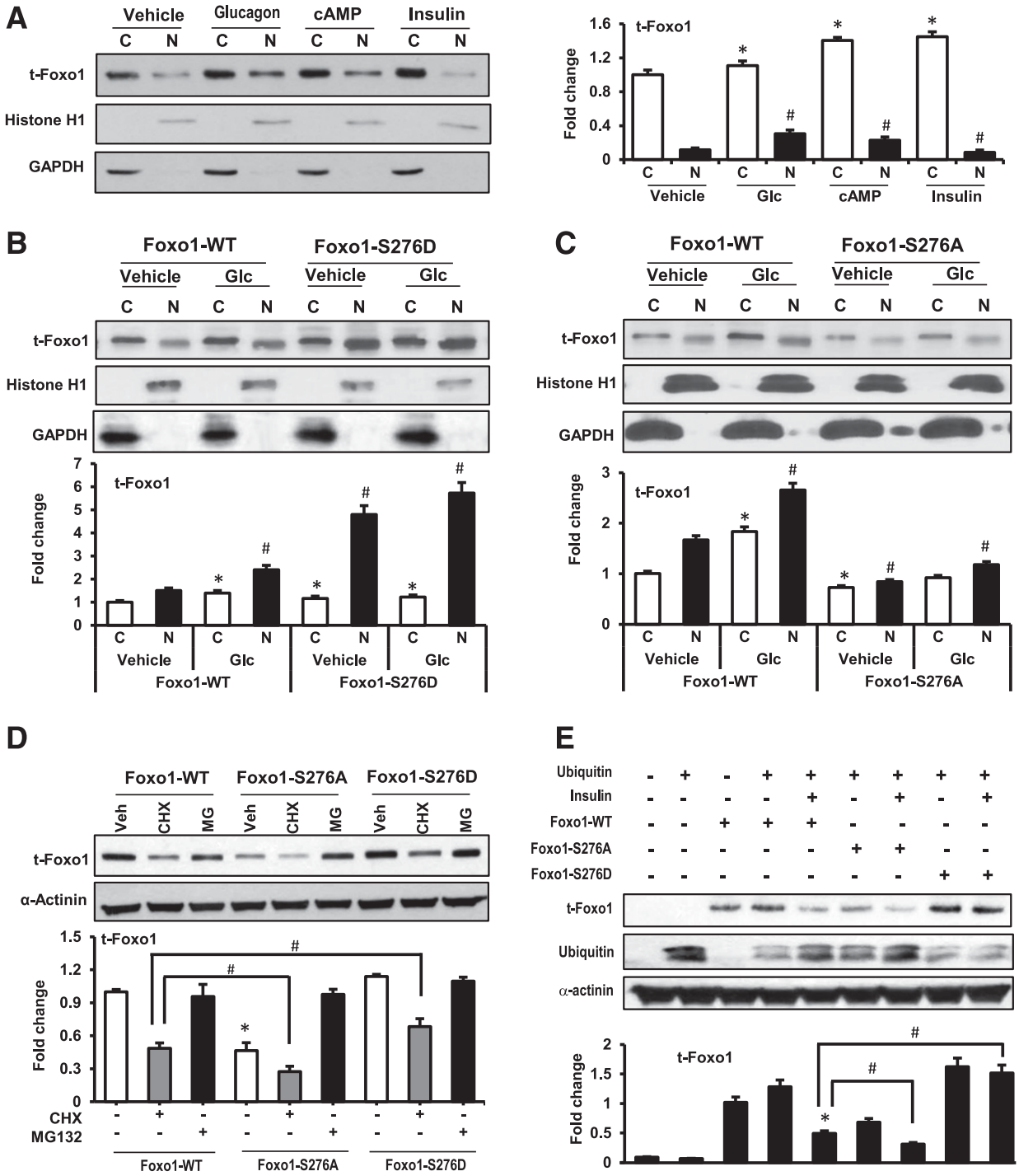

Figure 6—Glucagon or cAMP stimulates Foxo1 nuclear localization and Foxo1-S276 phosphorylation, enhancing Foxo1 stability in hepatocytes. *A*: HepG2 cells were transfected with 5 μg plasmid DNA expressing hemagglutinin (HA)-Foxo1 for 18 h and then treated with 100 nmol/L glucagon, 10 μmol/L cAMP, or 100 nmol/L insulin for 30 min prior to extraction of nuclear (N) and cytoplasmic (C) proteins. A total of 20 μg nuclear protein or 100 μg cytoplasmic protein was immunoblotted to determine the abundance of total Foxo1 (t-Foxo1) in nucleus or cytoplasm. Signal intensity was quantified by ImageJ software for statistical comparison. Cytoplasmic and nuclear protein levels were normalized by GAPDH and histone H1, respectively. $n = 3$ experiments. $^*P < 0.05$ vs. vehicle in cytoplasm; $\#P < 0.05$ vs. vehicle in nucleus. *B* and *C*: Distribution of Foxo1-S276 mutant proteins in the nucleus and cytoplasm of cells. HepG2 cells were transfected with 5 μg plasmid DNA expressing Foxo1-WT, S276A, or S276D for 18 h and then treated with or without 100 nmol/L glucagon (Glc) for 30 min. Nuclear (N) or cytoplasmic (C) protein was extracted to determine protein abundance of Foxo1-S276 mutants in nucleus and cytoplasm. Representative images are shown in *B* and *C*, and signal intensity was quantified by ImageJ software for statistical comparison. $n = 3$ experiments. $^*P < 0.05$ vs. vehicle in cytoplasm; $\#P < 0.05$ vs. vehicle in nucleus. *D*: Foxo1-S276 mutations influence Foxo1 stability in a proteasome-dependent manner. Western blotting was performed to detect t-Foxo1 abundance in HepG2 cells that was transfected with the same amount of plasmid DNA expressing Foxo1-WT, S276A, or S276D for 10 h, and cells were then starved for 8 h and treated with 10 μmol/L CHX or 10 μg/mL MG132 (MG) for 6 h prior cellular protein collection. Representative images are shown. Signal intensity was

transfected with Foxo1-WT, S276A, or S276D (Fig. 6*D*). Moreover, when Foxo1 protein synthesis was inhibited by CHX in cells, the remaining Foxo1 protein level in the Foxo1-S276D group increased by 40%, whereas it decreased by 44% in the Foxo1-S276A group compared with the Foxo1-WT group (Fig. 6*D*). These data suggest that Foxo1-S276 phosphorylation promoted Foxo1 stability, whereas nonphosphorylation of S276 enhanced 26S proteasome-dependent degradation of Foxo1.

Foxo1-S276 Phosphorylation Impairs Insulin-Induced Foxo1 Ubiquitination and Foxo1 Nuclear Export

We next determined whether Foxo1-S276 phosphorylation or Foxo1-S276D affects insulin-induced Foxo1 ubiquitination in cells. HepG2 cells were transfected with an equal amount of Foxo1-WT or S276D plasmid DNA together with ubiquitin for 10 h, then stimulated with insulin for an additional 12 h, and then total cellular proteins were extracted for analysis. Western blotting analysis revealed that insulin reduced total Foxo1 protein by 50% in Foxo1-WT– or S276A-expressed cells, whereas the effect of insulin was abolished in cells expressing Foxo1-S276D mutant (Fig. 6*E*).

We further assessed whether Foxo1-S276 phosphorylation or Foxo1-S276D affects insulin-induced Foxo1 nuclear translocation in cells. HepG2 cells were transfected with an equal amount of Foxo1-WT or S276D plasmid DNA for 18 h and then stimulated with insulin over a 120-min time course. Upon insulin stimulation for either 90 or 120 min, Foxo1-WT protein was primarily located in the cytoplasm (Fig. 7*A*–*C*). Foxo1-S276D protein primarily localized at both cytoplasm and nucleus with increased levels compared with Foxo1-WT. However, Foxo1-S276D largely blocked insulin-stimulated nuclear export, particularly at 120-min treatment of insulin (Fig. 7*A*), which was confirmed by Western blotting. Moreover, the blotting result showed that the cytoplasmic Foxo1-S256 phosphorylation by insulin for a 90- or 120-min treatment was significantly impaired by S276D mutation because the basal level of Foxo1-S256 phosphorylation was higher in S276D than WT in cells (Fig. 7*B* and *C*). These results reveal that Foxo1-S276 phosphorylation or aspartate mutation promoted Foxo1 nuclear localization and stability and impaired the ability of insulin to induce Foxo1 nuclear export and/or degradation, which may serve as a mechanism for insulin resistance at the Foxo1 level.

Foxo1-S273 Phosphorylation Controls Blood Glucose Homeostasis and Hepatic Glucose Production in Mice

To further explore the physiological function of equivalent human Foxo1-S276 in glucose metabolism in mice, we used the CRISPR/Cas9 approach to generate Foxo1-S273A and Foxo1-S273D KI mice, in which the endogenous Foxo1-S273 alleles were replaced by alanine (A) or aspartate (D) mutations (Supplementary Fig. 1). All of the mice survived with no obvious physiological deficiency. The feeding blood glucose increased by 20% in Foxo1-$S276^{D/D}$ mice, and there was no change in Foxo1-$S276^{A/A}$ mice compared with control. The fasting blood glucose increased by 31% in Foxo1-$S276^{D/D}$ mice but decreased significantly by 10% in Foxo1-$S276^{A/A}$ mice (Fig. 8*A*). Hepatic Igfbp-1 and G6pc mRNA expression significantly increased by 4.5- and 2.1-fold in the liver of Foxo1-$S273^{D/D}$ compared with control liver, respectively. However, there was a 25% reduction for both gene expression in $S273^{A/A}$ liver compared with control liver ($P < 0.05$) (Fig. 8*B*). The total Foxo1 protein level in the liver was increased by 2.6-fold in Foxo1-$S273^{D/D}$ mice, but reduced by 40% in Foxo1-$S273^{A/A}$ mice when compared with control ($P < 0.05$) (Fig. 8*C*).

We further assessed the direct role of Foxo1-S273 phosphorylation in control of HGP using the primary hepatocytes isolated from Foxo1-$S273^{A/A}$, $S273^{D/D}$, and WT mice. The basal level of HGP was increased by 46% in Foxo1-$S273^{D/D}$ hepatocytes, but the basal potential was reduced by 40% in Foxo1-$S273^{A/A}$ hepatocytes, compared with control hepatocytes ($P < 0.01$) (Fig. 8*D*). Upon glucagon stimulation, HGP was increased by 53% in control hepatocytes; however, this stimulatory effect was significantly impaired or attenuated by either Foxo1-S273D or S273A mutation, which exhibited an increase by 41% or 20%, respectively ($P < 0.01$) (Fig. 8*D*). Glucagon-stimulated glycogenolysis barely impaired by Foxo1 mutation in the cells.

We next performed glucagon tolerance tests in Foxo1-$S273^{A/A}$, $S273^{D/D}$, and WT mice in the fasting state. Both WT and Foxo1-$S273^{D/D}$ mice exhibited a 1.8-fold increase, and Foxo1-$S273^{A/A}$ mice had a 1.6-fold increase in blood glucose after 15 min of glucagon injection, indicating that Foxo1-$S273^{A/A}$ mutant impaired glucagon stimulation of blood glucose. Importantly, in WT and Foxo1-$S273^{A/A}$ mice, blood glucose returned to initial level 60 min after glucagon injection; however, high blood glucose level was maintained in Foxo1-$S273^{D/D}$ mice, indicating that Foxo1-$S273^{D/D}$ mutant prolonged glucagon stimulation of blood glucose ($P < 0.05$) (Fig. 8*E* and *F*). The impaired effects of glucagon stimulation on HGP and blood glucose by Foxo1 mutations at S273 suggest the important role of Foxo1-S273 phosphorylation plays in glucagon signaling in control of hepatic gluconeogenesis and blood glucose.

quantified and normalized by α-actinin for statistical analysis. *$P < 0.05$ vs. Foxo1-WT; #$P < 0.05$ for the comparison of designated groups. $n = 3$ different experiments. *E*: Foxo1-S276 mutations influence insulin-induced Foxo1 ubiquitination. HepG2 cells were cotransfected with eGFP expression vectors encoding WT Foxo1, Foxo1-S276D, or Foxo1-S276A and/or FLAG-ubiquitin for 10 h; cells were starved for 12 h and then treated with 100 nmol/L insulin for 12 h. Quantification of t-Foxo1 normalized by α-actinin was performed using ImageJ. *$P < 0.05$ vs. Foxo1-WT and FLAG-ubiquitin group; #$P < 0.05$ for comparison of designated groups. $n = 3$ different experiments.

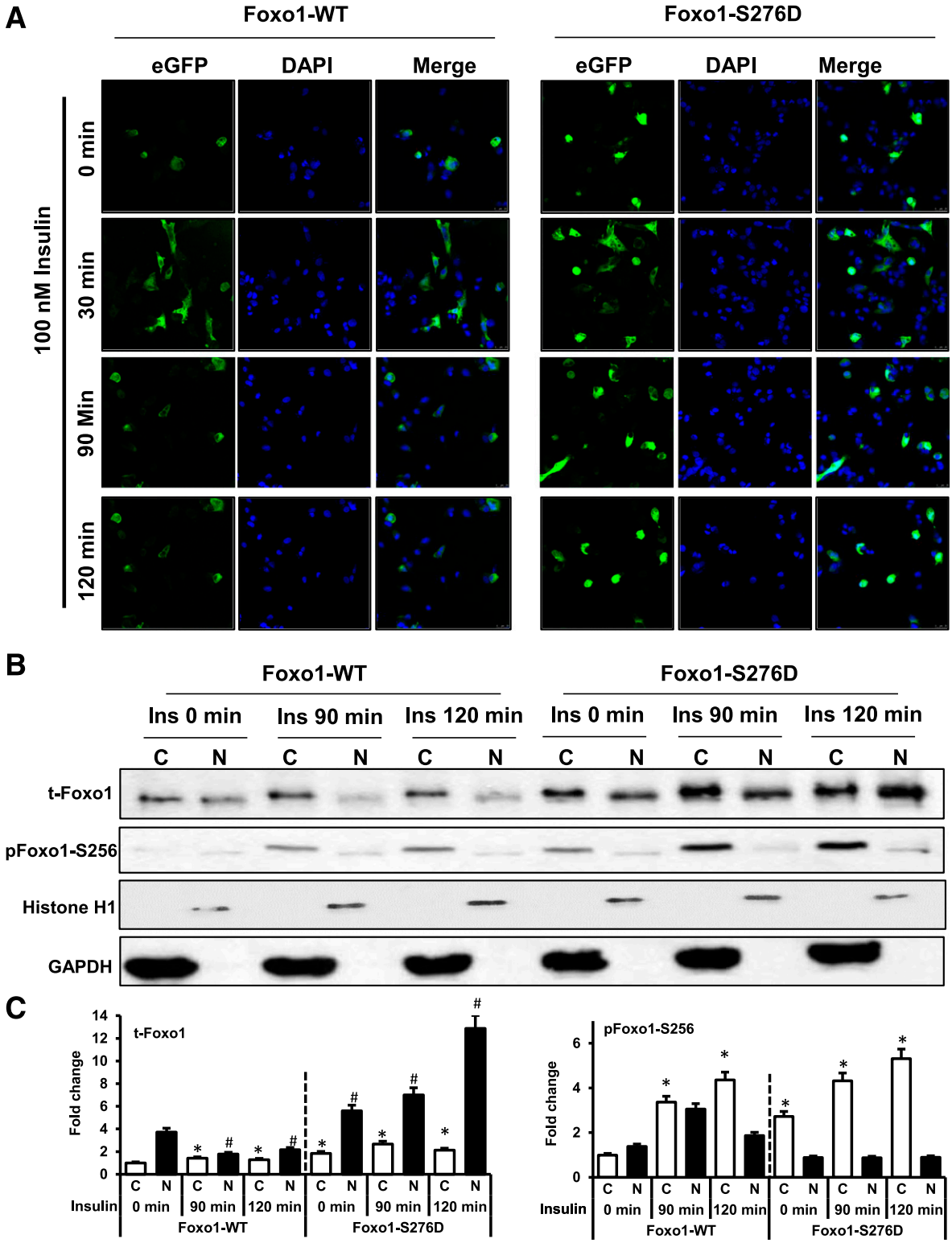

Figure 7—Foxo1-S276D impairs insulin-stimulated Foxo1 nuclear export in hepatocytes. *A*: HepG2 cells were transfected with 5 μg plasmid DNA expressing eGFP-Foxo1-WT or eGFP-Foxo1-S276D for 18 h, and cells were then serum starved for 8 h prior to 100 nmol/L insulin treatment for 0, 30, 90, or 120 min. The GFP-positive cells were displayed, stained with DAPI for nucleus, and analyzed under the confocal microscope. Representative images are shown. *B*: HepG2 cells were transfected with 10 μg eGFP expression vectors encoding Foxo1-WT or Foxo1-S276D for 18 h and followed by 8-h serum starvation prior to 100 nmol/L insulin (Ins) stimulation for 90 and 120 min. Western blotting was performed for total Foxo1 (t-Foxo1) and phosphorylated (p)Foxo1-S256 in cytoplasm (C) and nucleus (N). *C*: Quantification of t-Foxo1 and pFoxo1-S256/t-Foxo1 was performed by ImageJ. Cytoplasmic (C) and nuclear (N) protein levels were normalized by GAPDH and histone H1, respectively. Results are presented as mean ± SEM. $n = 3$ different experiments. *$P < 0.05$ vs. 0 min of insulin treatment from Foxo1-WT in cytoplasm; #$P < 0.05$ vs. 0 min of insulin treatment from Foxo1-WT in nucleus.

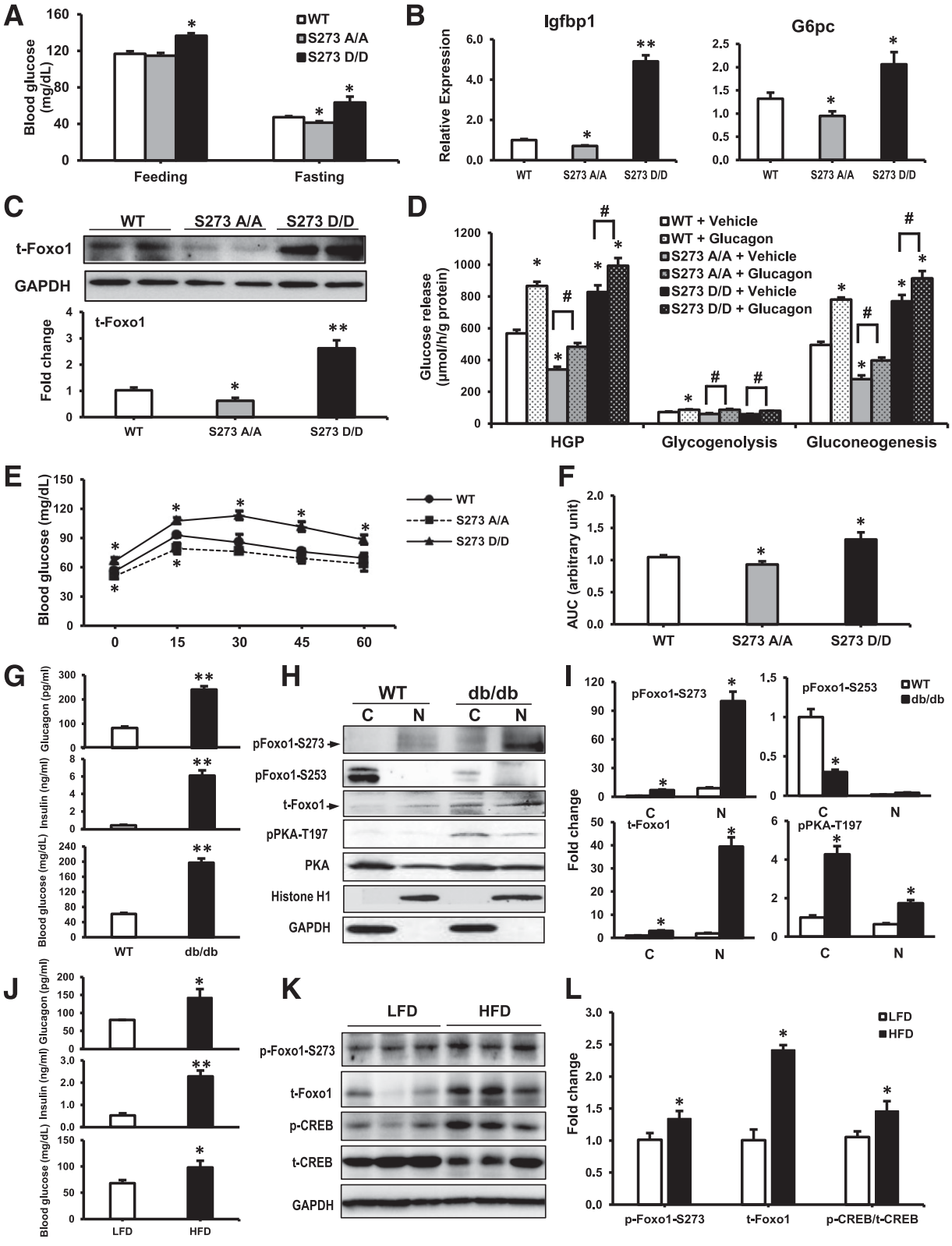

Figure 8— Foxo1-S273 mutations impair blood glucose and HGP in mice. *A*: Blood glucose levels of random-fed or 18-h–fasted mice. $n = 4$–6 mice/genotype. $^*P < 0.05$ vs. WT mice. *B*: Quantitative PCR analysis of expression of Igfbp-1 and G6pc in the liver of 18-h–fasted mice. $n = 4$ mice/genotype. $^*P < 0.05$; $^{**}P < 0.01$ vs. WT mice. *C*: Foxo1 protein levels in the livers of the mutant mice. Western blotting results from two mice per genotype are shown representatively. $^*P < 0.05$; $^{**}P < 0.01$ vs. WT. $n = 4$/group. *D*: HGP assays in the primary hepatocytes isolated from WT, Foxo1-S273$^{A/A}$, and Foxo1-S273$^{D/D}$ KI mice. Fresh hepatocytes were isolated from these mice, and HGP were measured 3 h after 100 nmol/L glucagon stimulation and normalized to total protein levels. $n = 3$/treatment. $^*P < 0.05$ vs. WT with vehicle group; $\#P < 0.05$ for the comparison of designated groups. *E* and *F*: Glucagon tolerance tests. *E*: Glucagon tolerance tests for mice after

Foxo1-S273 Phosphorylation Increases in the Liver of *db/db* and HFD-Fed Mice

Finally, we examined Foxo1-S273 phosphorylation in the liver of *db/db* diabetic mice, as well as HFD-induced insulin-resistant mice. The *db/db* mice exhibited elevations in blood glucagon, glucose, and serum insulin by 3-, 3-, and 10-fold, respectively, compared with control mice (Fig. 8*G*). Moreover, total Foxo1 protein and S273 phosphorylation significantly increased in the liver of *db/db* mice and accumulated in the nucleus (Fig. 8*H*). In parallel with increased Foxo1-S273 phosphorylation, PKA-T197 phosphorylation indicative of PKA activity was also markedly enhanced in both nucleus and cytoplasm in the liver of *db/db* mice (Fig. 8*I*). The HFD-fed mice exhibited increased blood glucagon, glucose, and serum insulin by 1.8-, 1.4-, and 5-fold, respectively, compared with LFD-fed mice (Fig. 8*J*). Moreover, total Foxo1 protein and Foxo1-S273 phosphorylation significantly increased in the liver of HFD-fed mice when compared with the LFD-fed liver (Fig. 8*K* and *L*). These data suggest that Foxo1-S273 phosphorylation and its nuclear retention, along with excess glucagon and PKA activity, coexist in the liver of animals with type 2 diabetes or insulin resistance.

DISCUSSION

We and other groups have previously established that insulin phosphorylates human Foxo1-S256 by activation of Akt that promotes Foxo1 cytoplasmic sequestration or nuclear export and then suppresses expression of genes responsible for HGP (12,18,20,21,35). In this study, using in vitro kinase assay–coupled LC-MS, phosphospecific antibodies, and CRISPR/Cas9-based Foxo1 KI mutant mice, we were able to identify a novel molecular, cellular, and physiological mechanism by which Foxo1 mediates glucagon signaling via phosphorylation at Ser^{276} (human) or Ser^{273} (mouse) in control of hepatic gluconeogenesis and blood glucose.

Glucagon has been implicated in the pathogenesis of diabetic hyperglycemia, largely by enhancing HGP, which is believed to be a key mechanism for pathogenesis of diabetes (36). In mice with type 2 diabetes, we recently demonstrated that hepatic Foxo1 deletion reduced HGP and blood glucose in *db/db* mice (16). Given that a high glucagon level is present in both types of diabetes (6), hyperactivation of Foxo1 by activated PKA and inactivated Akt upon insulin resistance or deficiency may serve as fundamental mechanisms for excess liver gluconeogenesis resulting in diabetic hyperglycemia.

The mechanism by which Foxo1-S276 phosphorylation promotes Foxo1 nuclear retention and stability is involved in the prevention of proteasome-mediated Foxo1 ubiquitination. We expect that Foxo1-S276 phosphorylation might enhance its recruitment with a number of cofactors, such as importin or CREB, to participate in Foxo1 subcellular trafficking and gene transcription, but detailed molecular aspects warrant further investigation. By activating heterologous signaling cascades, glucagon primarily activates PKA and downstream effectors, including glycogen phosphorylase for glycogenolysis and CREB for gluconeogenesis (9,37). Glucagon also minimally activates Akt phosphorylation, but its duration and intensity seemed insufficient for induction of Foxo1-S256 phosphorylation and degradation (Fig. 2). Thus, insulin is a major hormone for the endogenous Akt activation downstream of the IRS1- and 2-associated phosphoinositide 3-kinase, as we observed in the liver or heart of male mice (15,26,38). In this study, our in vitro data established that Foxo1-S276 is a target of PKA in glucagon signaling and promotes Foxo1 nuclear retention. Foxo1-S276D mutation mimics Foxo1-S276 phosphorylation and promotes Foxo1 nuclear localization and stability. Moreover, Foxo1-S273D mutation impairs the ability of insulin-stimulated Foxo1 nuclear export or cytoplasmic sequestration. This finding suggests a novel mechanism for insulin resistance when Foxo1-S273 is phosphorylated. Conversely, Foxo1-S276A mutation, which blocks phosphorylation, enhances Foxo1 ubiquitination and/or degradation, a process reversed by the 28*S* proteasome inhibitor MG132. This study reveals a unique mechanism of Foxo1 regulation by which glucagon stimulates HGP via Foxo1 at the posttranslational level.

Foxo1 can be regulated by multiple protein kinases (15). It has been shown that mitogen-activated protein kinase phosphorylates Foxo1 at S246, S284, S295, S326, S413, S415, S429, S467, S475, and T557, and p38α phosphorylates 5 of the 10 sites: S284, S295, S326, S467, and S475 (39). Moreover, these phosphorylation sites are shared by CaMKII, expression of a Foxo1-S7A mutation (S246A/S284A/S295A/S413A/S415A/S429A/S475A) attenuated glucagon-induced Foxo1 nuclear localization, and it is suggested that CaMKII promotes Foxo1 nuclear localization through p38α activation that stimulates hepatic gluconeogenesis (24,40). The Foxo1-S273 phosphorylation

an 18-h overnight fast. Blood glucose levels (mean ± SEM) were determined at the indicated time points after i.p. injection of 16 μg/kg body weight glucagon. $n = 6$ mice. $^*P < 0.05$ vs. WT. *F*: Area under the curve (AUC) from *E* was calculated. $^*P < 0.05$ vs. WT. $n = 4$–6/group. *G*: Blood glucagon, insulin, and glucose levels in WT and *db/db* mice in an 18-h fasting state. $^{**}P < 0.01$ vs. WT. $n = 4$ mice/group. *H*: Phosphorylated (p)Foxo1-S273, pFoxo1-S253, total Foxo1 (t-Foxo1), pPKA-T179, PKA, histone H1, and GAPDH in 100 μg cytoplasmic protein (C) and 20 μg nuclear protein (N) of mouse livers were determined by Western blotting. *I*: Quantification of pFoxo1-S273, pS253, t-Foxo1, pPKA-T197, or PKA was performed by ImageJ. The cytoplasmic (C) and nuclear (N) protein levels were normalized by GAPDH and histone H1, respectively. $^*P < 0.05$ vs. WT. $n = 3$ mice/group. Results are shown as mean ± SEM. *J*: Blood glucagon, insulin, and glucose levels in LFD- and HFD-fed WT mice in an 18-h fasting state. $^*P < 0.05$; $^{**}P < 0.01$ vs. LFD. $n = 4$/group. *K*: pFoxo1-S273, t-Foxo1, pCREB, and CREB levels of mouse livers were determined by Western blotting. *L*: Quantification of pFoxo1-S273, t-Foxo1, pCREB, and CREB was performed by ImageJ. $^*P < 0.05$ vs. LFD. $n = 4$ mice/group. Results are shown as mean ± SEM.

identified as a target of PKA is distinct from these sites, but whether it is involved by other protein kinases, such as p38α, remains to be determined.

HGP is generally regulated by direct mechanisms of insulin action in hepatocytes autonomously (41). Our early studies suggest that direct hepatocytes signaling via IRS1- and 2-mediated Akt activation or hepatic Foxo1 suppression is required for hepatic insulin suppression on HGP and blood glucose (26). However, a recent report (42) suggests that an indirect insulin that suppresses free fatty acid influx to hepatocytes from lipolysis of adipose tissue is critical for suppression of HGP so that hepatocyte Akt signaling is dispensable for HGP suppression. Indeed, HGP can be regulated by indirect insulin action in extrahepatic tissues nonautonomously (41). In addition, to suppress glucagon secretion from pancreatic α-cells or antagonize the effect of cAMP, insulin also suppresses HGP by the central nervous system in hypothalamic neurons via a vagal efferent (43). Thus, we do not rule out the possibility of other tissues including the central nervous system, adipose tissue, and pancreas on HGP control in the L-F1KO and KI mouse models, but our data from mouse primary hepatocytes do support that the cellular autonomous effect of glucagon in hepatocytes has critical roles in controlling Foxo1, gluconeogenesis, and HGP.

Foxo1 has a variety of target genes responsible for multiple physiological functions in the body (11,15,44, 45). We have recently identified two other Foxo1 target genes in the liver, such as angiotensinogen, a precursor of angiotensin II that regulates blood pressure (44). Foxo1 also promotes expression of heme oxygenase-1, reducing synthesis of heme and mitochondria (46) and driving bodily metabolic inflammation and insulin resistance in mice and humans (47). In this study, we demonstrated a novel regulatory mechanism of Foxo1 by glucagon-cAMP–PKA signaling in hepatocytes, but we do not rule out the possibility of a similar Foxo1 regulation by other hormones via activation of PKA in tissues, including but not limited to glucagon (48). Indeed, hormones such as catecholamines or glucocorticoids also increase hepatic gluconeogenesis or promote insulin resistance under certain conditions involving activation of PKA, such as stress (49). Our studies demonstrate that Foxo1 is a mediator of multiple signaling cascades (e.g., PKA and Akt); it integrates different hormones and intracellular protein kinases into the nuclear gene transcriptional programming in control of insulin sensitivity, HGP, and blood glucose. Thus, Foxo1-S276 phosphorylation may not only serve as a novel and important biomarker for Foxo1 stability and bioactivity contributing to hyperglycemia upon development of diabetes, but also provides a potential therapeutic target in control of Foxo1 stability and activity to prevent diabetes and associated diseases in the future.

Acknowledgments. The authors thank Mike Honig, who provided English editing for the manuscript. S.G. also thanks the scientists at Covance (Denver, PA) and Cyagen Biosciences (Santa Clara, CA) for help generating Foxo1-phosphospecific antibodies and KI mice, respectively.

Funding. This study was supported by grants from the National Institutes of Health (R01-DK-095118), American Diabetes Association Career Development Award (1-15-CD-09) and Minority Undergraduate Internship Award (1-17-MUI-008), the American Heart Association (BGIA-7880040), a Faculty Startup from the Texas A&M University Health Science Center and AgriLife Research, and the U.S. Department of Agriculture National Institute of Food and Agriculture (Hatch 1010958) to S.G. S.G. is the recipient of the 2015 American Diabetes Association Research Excellence Thomas R. Lee Award.

Duality of Interest. No potential conflicts of interest relevant to this article were reported.

Author Contributions. Y.W., Q.P., H.Y., K.Z., X.G., Z.X., W.Y.,Y.Q., C.A.G., C.H., L.Z., A.Z., L.L., and Y.C. performed experiments. Y.W., Q.P., H.Y., and S.G. wrote the manuscript. L.Z. and A.Z. performed LC-MS and analyzed the data. W.Z., Y.S., H.Z., F.W., and L.H. analyzed and interpreted data. S.G. conceived of the hypothesis and designed the experiments. S.G. is the guarantor of this work and as such, had full access to all of the data in the study and takes responsibility for the integrity of the data and accuracy of the data analysis.

Prior Presentation. Parts of this study were presented at the 75th Scientific Sessions of the American Diabetes Association, Boston, MA, 5–9 June 2015 and the 78th Scientific Sessions of the American Diabetes Association, Orlando, FL, 22–26 June 2018.

References

1. Ali S, Drucker DJ. Benefits and limitations of reducing glucagon action for the treatment of type 2 diabetes. Am J Physiol Endocrinol Metab 2009;296: E415–E421

2. Edgerton DS, Cherrington AD. Glucagon as a critical factor in the pathology of diabetes. Diabetes 2011;60:377–380

3. Unger RH. Glucagon physiology and pathophysiology. N Engl J Med 1971; 285:443–449

4. Tahrani AA, Bailey CJ, Del Prato S, Barnett AH. Management of type 2 diabetes: new and future developments in treatment. Lancet 2011;378:182–197

5. Johnson DG, Goebel CU, Hruby VJ, Bregman MD, Trivedi D. Hyperglycemia of diabetic rats decreased by a glucagon receptor antagonist. Science 1982; 215:1115–1116

6. Lee Y, Wang MY, Du XQ, Charron MJ, Unger RH. Glucagon receptor knockout prevents insulin-deficient type 1 diabetes in mice. Diabetes 2011;60:391–397

7. Lund A, Bagger JI, Wewer Albrechtsen NJ, et al. Evidence of extrapancreatic glucagon secretion in man. Diabetes 2016;65:585–597

8. Mayr B, Montminy M. Transcriptional regulation by the phosphorylation-dependent factor CREB. Nat Rev Mol Cell Biol 2001;2:599–609

9. An H, He L. Current understanding of metformin effect on the control of hyperglycemia in diabetes. J Endocrinol 2016;228:R97–R106

10. He L, Sabet A, Djedjos S, et al. Metformin and insulin suppress hepatic gluconeogenesis through phosphorylation of CREB binding protein. Cell 2009;137: 635–646

11. Accili D, Arden KC. FoxOs at the crossroads of cellular metabolism, differentiation, and transformation. Cell 2004;117:421–426

12. Guo S, Rena G, Cichy S, He X, Cohen P, Unterman T. Phosphorylation of serine 256 by protein kinase B disrupts transactivation by FKHR and mediates effects of insulin on insulin-like growth factor-binding protein-1 promoter activity through a conserved insulin response sequence. J Biol Chem 1999;274:17184–17192

13. O'Brien RM, Lucas PC, Forest CD, Magnuson MA, Granner DK. Identification of a sequence in the PEPCK gene that mediates a negative effect of insulin on transcription. Science 1990;249:533–537

14. Onuma H, Vander Kooi BT, Boustead JN, Oeser JK, O'Brien RM. Correlation between FOXO1a (FKHR) and FOXO3a (FKHRL1) binding and the inhibition of basal glucose-6-phosphatase catalytic subunit gene transcription by insulin. Mol Endocrinol 2006;20:2831–2847

15. Guo S. Insulin signaling, resistance, and the metabolic syndrome: insights from mouse models into disease mechanisms. J Endocrinol 2014;220:T1–T23
16. Zhang K, Li L, Qi Y, et al. Hepatic suppression of Foxo1 and Foxo3 causes hypoglycemia and hyperlipidemia in mice. Endocrinology 2012;153:631–646
17. Altomonte J, Richter A, Harbaran S, et al. Inhibition of Foxo1 function is associated with improved fasting glycemia in diabetic mice. Am J Physiol Endocrinol Metab 2003;285:E718–E728
18. Rena G, Guo S, Cichy SC, Unterman TG, Cohen P. Phosphorylation of the transcription factor forkhead family member FKHR by protein kinase B. J Biol Chem 1999;274:17179–17183
19. Dong XC, Copps KD, Guo S, et al. Inactivation of hepatic Foxo1 by insulin signaling is required for adaptive nutrient homeostasis and endocrine growth regulation. Cell Metab 2008;8:65–76
20. Nakae J, Park BC, Accili D. Insulin stimulates phosphorylation of the forkhead transcription factor FKHR on serine 253 through a Wortmannin-sensitive pathway. J Biol Chem 1999;274:15982–15985
21. Biggs WH III, Meisenhelder J, Hunter T, Cavenee WK, Arden KC. Protein kinase B/Akt-mediated phosphorylation promotes nuclear exclusion of the winged helix transcription factor FKHR1. Proc Natl Acad Sci U S A 1999;96:7421–7426
22. Schmoll D, Walker KS, Alessi DR, et al. Regulation of glucose-6-phosphatase gene expression by protein kinase Balpha and the forkhead transcription factor FKHR. Evidence for insulin response unit-dependent and -independent effects of insulin on promoter activity. J Biol Chem 2000;275:36324–36333
23. Yeagley D, Guo S, Unterman T, Quinn PG. Gene- and activation-specific mechanisms for insulin inhibition of basal and glucocorticoid-induced insulin-like growth factor binding protein-1 and phosphoenolpyruvate carboxykinase transcription. Roles of forkhead and insulin response sequences. J Biol Chem 2001; 276:33705–33710
24. Ozcan L, Wong CC, Li G, et al. Calcium signaling through CaMKII regulates hepatic glucose production in fasting and obesity. Cell Metab 2012;15: 739–751
25. Paik JH, Kollipara R, Chu G, et al. FoxOs are lineage-restricted redundant tumor suppressors and regulate endothelial cell homeostasis. Cell 2007;128:309–323
26. Guo S, Copps KD, Dong X, et al. The Irs1 branch of the insulin signaling cascade plays a dominant role in hepatic nutrient homeostasis. Mol Cell Biol 2009; 29:5070–5083
27. Wang H, Yang H, Shivalila CS, et al. One-step generation of mice carrying mutations in multiple genes by CRISPR/Cas-mediated genome engineering. Cell 2013;153:910–918
28. Rossi M, Zhu L, McMillin SM, et al. Hepatic Gi signaling regulates whole-body glucose homeostasis. J Clin Invest 2018;128:746–759
29. Guo S, Dunn SL, White MF. The reciprocal stability of FOXO1 and IRS2 creates a regulatory circuit that controls insulin signaling. Mol Endocrinol 2006;20:3389–3399
30. Chen Z, Sheng L, Shen H, et al. Hepatic TRAF2 regulates glucose metabolism through enhancing glucagon responses. Diabetes 2012;61:566–573
31. Sun Z, Miller RA, Patel RT, et al. Hepatic Hdac3 promotes gluconeogenesis by repressing lipid synthesis and sequestration. Nat Med 2012;18:934–942
32. Zhang X, Gan L, Pan H, et al. Phosphorylation of serine 256 suppresses transactivation by FKHR (FOXO1) by multiple mechanisms. Direct and indirect effects on nuclear/cytoplasmic shuttling and DNA binding. J Biol Chem 2002;277: 45276–45284
33. Matsumoto M, Pocai A, Rossetti L, Depinho RA, Accili D. Impaired regulation of hepatic glucose production in mice lacking the forkhead transcription factor Foxo1 in liver. Cell Metab 2007;6:208–216
34. Gromada J, Duttaroy A, Rorsman P. The insulin receptor talks to glucagon? Cell Metab 2009;9:303–305
35. Huang H, Regan KM, Wang F, et al. Skp2 inhibits FOXO1 in tumor suppression through ubiquitin-mediated degradation. Proc Natl Acad Sci U S A 2005; 102:1649–1654
36. Unger RH, Cherrington AD. Glucagonocentric restructuring of diabetes: a pathophysiologic and therapeutic makeover. J Clin Invest 2012;122:4–12
37. Altarejos JY, Montminy M. CREB and the CRTC co-activators: sensors for hormonal and metabolic signals. Nat Rev Mol Cell Biol 2011;12:141–151
38. Qi Y, Xu Z, Zhu Q, et al. Myocardial loss of IRS1 and IRS2 causes heart failure and is controlled by p38α MAPK during insulin resistance. Diabetes 2013;62: 3887–3900
39. Asada S, Daitoku H, Matsuzaki H, et al. Mitogen-activated protein kinases, Erk and p38, phosphorylate and regulate Foxo1. Cell Signal 2007;19:519–527
40. Cao W, Collins QF, Becker TC, et al. p38 Mitogen-activated protein kinase plays a stimulatory role in hepatic gluconeogenesis. J Biol Chem 2005;280: 42731–42737
41. Cherrington AD, Edgerton D, Sindelar DK. The direct and indirect effects of insulin on hepatic glucose production in vivo. Diabetologia 1998;41:987–996
42. Titchenell PM, Quinn WJ, Lu M, et al. Direct hepatocyte insulin signaling is required for lipogenesis but is dispensable for the suppression of glucose production. Cell Metab 2016;23:1154–1166
43. Myers MG Jr., Olson DP. Central nervous system control of metabolism. Nature 2012;491:357–363
44. Qi Y, Zhang K, Wu Y, et al. Novel mechanism of blood pressure regulation by forkhead box class O1-mediated transcriptional control of hepatic angiotensinogen. Hypertension 2014;64:1131–1140
45. Ren H, Orozco IJ, Su Y, et al. FoxO1 target Gpr17 activates AgRP neurons to regulate food intake. Cell 2012;149:1314–1326
46. Cheng Z, Guo S, Copps K, et al. Foxo1 integrates insulin signaling with mitochondrial function in the liver. Nat Med 2009;15:1307–1311
47. Jais A, Einwallner E, Sharif O, et al. Heme oxygenase-1 drives metaflammation and insulin resistance in mouse and man. Cell 2014;158:25–40
48. Zhang X, Szeto C, Gao E, et al. Cardiotoxic and cardioprotective features of chronic β-adrenergic signaling. Circ Res 2013;112:498–509
49. McGuinness OP, Shau V, Benson EM, et al. Role of epinephrine and norepinephrine in the metabolic response to stress hormone infusion in the conscious dog. Am J Physiol 1997;273:E674–E681